Cage Compounds

International Edition: DOI: 10.1002/anie.201502912
German Edition: DOI: 10.1002/ange.201502912

A Porous Tricyclooxacalixarene Cage Based on Tetraphenylethylene**

Chun Zhang, Zhen Wang, Liangxiao Tan, Tian-Long Zhai, Sheng Wang,* Bien Tan,* Yan-Song Zheng,* Xiang-Liang Yang, and Hui-Bi Xu*

Abstract: *A quadrangular prismatic tricyclooxacalixarene cage **1** based on tetraphenylethylene (TPE) was efficiently synthesized by a one-pot S_NAr condensation reaction. As a result of the porous internal structure in the solid state, cage **1** exhibited a good CO_2 uptake capacity of 12.5 wt% and a high selectivity for CO_2 over N_2 adsorption of 80 (273 K, 1 bar) with a BET surface area of 432 $m^2 g^{-1}$. Formation of cage **1** led to the fluorescence of TPE being switched on in solution. The system was employed as a single-molecule platform to study the mechanism of aggregation-induced emission (AIE) by examining the restriction of intramolecular rotation (RIR).*

Rapid progress in organic porous materials has resulted in the development of different classes of porous networks, such as covalent organic frameworks (COFs)[1] and amorphous microporous organic polymers.[2,3] Interest has grown in the development of porous materials composed of single organic molecules with open structures (such as tris(o-phenylenedioxy)cyclotriphosphazene (TPP),[4] 3,3′,4,4′-tetra(trimethylsilylethynyl)biphenyl (TTEB),[5] the hydrogen-bonded organic framework HOF-1a,[6] and the supramolecular organic framework SOF-1a[7]) or closed structure (such as calixarenes,[8] and cucurbituril[9]) because of their intriguing solution-processible properties. To obtain permanent porosity, porous molecular crystals containing rotors[10] or porous cages with inherent internal voids[11] have been developed.

[*] Dr. C. Zhang, Z. Wang, T.-L. Zhai, Dr. S. Wang, Prof. X.-L. Yang, Prof. H.-B. Xu
College of Life Science and Technology
National Engineering Research Center for Nanomedicine
Huazhong University of Science and Technology
1037 Luoyu Road, Wuhan, 430074 (China)
E-mail: chunzhang@hust.edu.cn
shengwang@hust.edu.cn
L. Tan, Prof. B. Tan, Prof. Y.-S. Zheng
School of Chemistry and Chemical Engineering
Huazhong University of Science and Technology
1037 Luoyu Road, Wuhan, 430074 (China)
E-mail: bien.tan@hust.edu.cn
zyansong@hotmail.com

[**] This work is supported by the National Natural Science Foundation of China (20902031 and J1103514), the National Basic Research Program (2012CB932500), and the Fundamental Research Funds for the Central Universities (HUST 2015TS086). We thank the Analytical and Testing Center of the Huazhong University of Science and Technology for related analysis. We also thank Dr. Anthony F. Cozzolino (Assistant Professor, Chemistry and Biochemistry Texas Tech University) for the details of calculations with ORCA.

Supporting information for this article is available on the WWW under http://dx.doi.org/10.1002/anie.201502912.

Three-dimensional (3D) shape-persistent cage compounds[11] have attracted considerable attention because of their fascinating structures and potential application in gas storage, separation, host–guest chemistry, and catalysis.[12] So far, different synthetic methods to prepare cage compounds have been developed. For example, dynamic covalent chemistry (DCC)[13] has been used as a powerful approach towards cage formation using imine chemistry or boronic acid condensation and led to a series of important results.[14–19] To avoid the issue of the facile hydrolysis of linkages of imine or B–O bonds, ethynylene linkages have been used to construct stable cages by Sonogashira reactions,[20] Glaser-type coupling[21] or alkyne metathesis.[22] However, these methods have been somewhat restricted by the requirement for multiple reaction steps and the use of heavy metal catalysts. Therefore, the development of straightforward, cost-effective, and environmentally-friendly methods to prepare stable organic molecular cages is still important in the field of porous materials.

The nucleophilic aromatic substitution (S_NAr) reaction has been successfully utilized in the synthesis of oxacalixarenes,[23–26] which was recognized as a new generation of macrocyclic host molecules in supramolecular chemistry. Bicyclooxacalixarene [2+3] cages have also been constructed by S_NAr reactions of phloroglucin with nucleophilic reagents for application in host–guest chemistry.[27] However, the internal cavity is too small, which greatly limits their further applications, especially in gas storage. Using building blocks of a larger size to construct expanded oxacalixarene cages might facilitate their application in gas storage. However, the synthesis of larger and more complex multi-cyclooxacalixarene cages is still a challenge and remains largely unexplored.[28]

Tetraphenylethylene and its derivatives (TPEs)[29] have attracted increasing interest in photoelectric materials[30] and in chemo/biosensors[31] because they exhibit aggregation-induced emission (AIE), an effect based on the restriction of intramolecular rotation (RIR). Intensive efforts have been made to understanding the mechanism of RIR. Host–guest inclusions have been used to limit the motions of TPE by Tang et al.[32] and Zheng and co-workers,[33] respectively. Jiang et al. demonstrated restriction of the rotation of TPE in an intermolecular network to afford emissive conjugated microporous polymers.[34] Dincă et al. reported the immobilization of TPE units in a rigid metal–organic framework (MOF) through coordination polymerization in which TPE fluorescence was switched on.[35] All these efforts, however, are focused on the polymer or supramolecular systems. Although simple TPE molecular models based on a single-molecule platform are better to investigate structure–property relationships and to understand the AIE/RIR mechanism, the

examples are scattered.[36] We envisaged that introducing TPE units into a closed molecular system such as cage might offer a novel single-molecule platform to understand the RIR mechanism of AIE, and also might provide a porous fluorescent cage suitable for gas storage. To date, no such TPE-based cages have been reported.

Recently, we have used TPE as a building block to construct an expanded oxacalixarene and found that the TPE-based oxacalixarene adopts a 1,3-alternate conformation in which the TPE aromatic rings are nearly parallel, which suggested that the pendant phenols on TPE could be linked into a cage structure by two additional molecular linkers.[37] Herein, we report the synthesis of a tricyclooxacalixarene cage **1** by a one-pot S_NAr reaction of tetrahydroxytetraphenylethylene **2** with 2,6-dichloropyridine-3,5-dicarbonitrile (**3**). In the cage structure, two TPE units were locked in a rigid cage framework and the fluorescence of TPE was switched on in solution. The obtained tricyclic cage **1** assembled into a grid-like porous structure and displayed high adsorption capacity for CO_2, with extraordinarily high selectivity of CO_2/N_2.

The synthesis of the TPE-based tricyclooxacalixarene cage **1** was carried out by one-pot condensation reaction as depicted in Scheme 1. Tetrahydroxytetraphenylethylene **2** was prepared according to a reported method.[33] The coupling reaction of **2** with **3** in the presence of Cs_2CO_3 in DMSO at 25 °C for 4 h resulted in the formation of **1** which was isolated in a yield of 21 %.

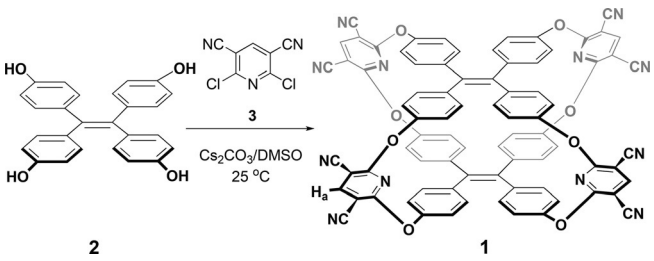

Scheme 1. Synthesis of TPE-based tricyclooxacalixarene cage **1**.

The structure of cage **1** was confirmed by single-crystal X-ray analysis.[42] Single crystals suitable for X-ray diffraction were obtained through recrystallization by cooling the hot DMSO solution of cage **1** to room temperature. As shown in Figure 1, tricyclic cage **1** crystallizes in an orthorhombic space group $Pna2_1$ and adopts a quadrangular prismatic structure with a large central cavity. As a result of the steric effect of the cage framework, the TPE units exhibited propeller-like and nonplanar conformations and resulted in the molecular cage being asymmetric. Four pyridine rings form four identical V-shaped clefts. In the prism structure, the distance between the top and bottom TPE is about 5.3 Å and the distance between the two pyridine ring N atoms in oppositely facing rings is about 7.4 Å (Figure S2a in the Supporting Information). Moreover, as a result of π···π ($d_{\pi\cdots\pi}$ = 3.54 and 3.57 Å) stacking and C–H···N ($d_{C-H\cdots N}$ = 2.73 and 2.63 Å) interactions, cage **1** packs to form a grid-like porous structure with a diameter of 11.83 Å (Figure S2b).

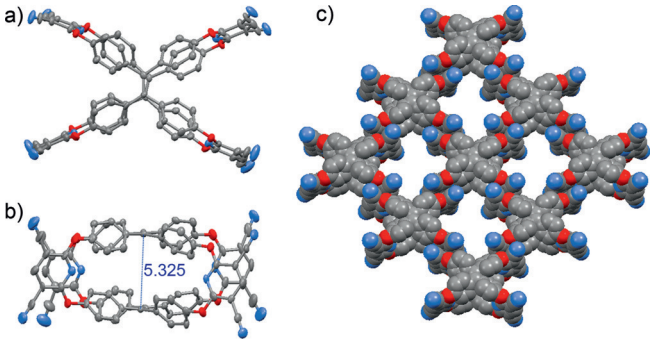

Figure 1. a) Top view and b) side view of the X-ray crystal structure of cage **1**. c) Grid-like porous structure from the crystal packing of cage **1** shown in space-filling mode. Hydrogen atoms and solvent molecule were omitted for clarity. Thermal ellipsoids in (a) and (b) are set at 50% probability. Atom colors: C = gray; N = blue; O = red.

The ^1H NMR spectrum of **1** in [D_6]DMSO (Figure S3) shows one singlet at δ = 9.03 ppm for the proton H_a of the pyridine moiety and a complicated set of signals for aromatic protons in the TPE scaffold at room temperature. Moreover, the ^{13}C NMR spectrum of cage **1** also showed complicated carbon resonances in [D_6]DMSO at room temperature (Figure S4). The complex proton and carbon resonance signals in the NMR spectra suggested that the symmetric structure of cage **1** was probably not retained in solution at room temperature. This distortion from symmetry is likely because of the steric strain on the TPE units caused by incorporation into the cage framework, which is consistent with its crystal structure (Figure 1). Variable-temperature NMR (VT-NMR) experiments were used to investigate the conformation of cage **1**. As shown in Figure S5, upon heating to 328 K, the signals attributable to the aromatic protons in TPE merged to form a single broad resonance signal. Further increasing the temperature led to the detection of a single sharper signal for the aromatic protons in TPE. These results indicated a fixed conformation of the cage at room temperature because of the tension and the steric effect. When the temperature was elevated, rapid interconversion of conformational isomers occurred, most likely as a result of the accelerated rotation of the phenyl rings on the NMR timescale. Based on the results of VT-NMR experiments, the activation energy ($\Delta G^{\neq}$) for the rotation of the phenyl ring was calculated to be 68 kJ mol^{-1}.[38]

Unlike TPE which shows no fluorescence in solution, cage **1** emits blue fluorescence at λ = 450 nm with a fluorescent quantum yield of 7.8 % when excited at λ = 320 nm in THF (see Figure S6 for the UV/Vis absorption spectra and Figure S7 for the fluorescence spectra). Like conventional fluorophores, cage **1** displays a visible solvent effect in solution. As shown in Figure S7, the fluorescence intensity of cage **1** decreased with increasing solvent polarity. Moreover, **1** exhibits a unique AIE effect. With the water fraction was increased from 0 to 60 %, the fluorescence intensity decreased. However, further increasing the water fraction dramatically enhanced the fluorescence intensity (Figure S7b and Figure S7c). The change of the intensity of fluorescence can be explained as follows. Upon addition of water into THF, the increase in solvent polarity quenched the fluorescence of

cage **1** because of the solvent effect. When the water fraction was increased to 70%, cage **1** precipitated from solution and was found to be highly fluorescent as a result of the AIE effect. Moreover, the fluorescence quantum yield for cage **1** in a mixture of 90% water/THF can be measured to 32.7%. Given these results, the TPE-based tricyclic cage **1** can be viewed as a useful single-molecule platform to investigate the RIR mechanism.

To understand the origin of the suppression of the phenyl ring rotation, quantum chemistry calculations based on density functional theory (DFT) were employed to explore the activation barrier for phenyl-ring flipping in cage **1**. The potential energy surface (PES) was constructed by varying the C_{Ar}–C_{Ar}–C=C dihedral angle from 0 to 180°. This process led to the rotation of just one phenyl ring along its symmetric axis while the other components of the system remained fixed (Figure 2a and b). From the PES pathway, the activation energy for the flipping of one phenyl ring in cage **1** was 73 kJ mol^{-1} (Figure 2c), which is higher than that of the TPE-MOF reported by Dincă et al. (49 kJ mol^{-1}) and TPE (24 kJ mol^{-1}) by 24 and 49 kJ mol^{-1} (Figure S8), respectively.[35b] The distances between hydrogen atoms was analyzed for cage **1** during the PES scanning process. As shown in Figure 2a,b and Figure S9, two very short distances were calculated in cage **1** for the H10–H84 and H5–H48 distances which measured 2.1 Å, which also demonstrated the significant steric hindrance in cage **1** (note: H48 is equivalent to H84 but is located at the back of the structure). The high activation barrier of phenyl ring flipping in cage **1** (73 kJ mol^{-1}) might be as a result of the steric effect based on the distortion of the geometry of the TPE units by the cage framework. As shown in Figure 3c, the lowest energy structure at the bottom of the PES is located at a C_{Ar}–C_{Ar}–C=C dihedral angle of 46.5°, which is very close to the crystallographic analysis in which the bond measured 46.3° (Figure S10). With the high activation barrier for phenyl ring flipping, non-radiative decay of the singlet excited state is decreased and therefore the fluorescence of TPE in dilute solution is enhanced.

Given the internal grid-like porous structure of cage **1** in the solid state, the gas adsorption and desorption properties of the structure were investigated (Figure 3). In preparation for these experiments, cage **1** was desolvated at 200°C for 8 h under vacuum until all DMSO had been removed (Figure S11). From the results of nitrogen sorption analysis, the BET surface area is 432 m^2 g^{-1} (the Langmuir surface area is 507 m^2 g^{-1}) and the total volume is 0.23 cm^3 g^{-1}. A steep nitrogen gas uptake at low relative pressure in the

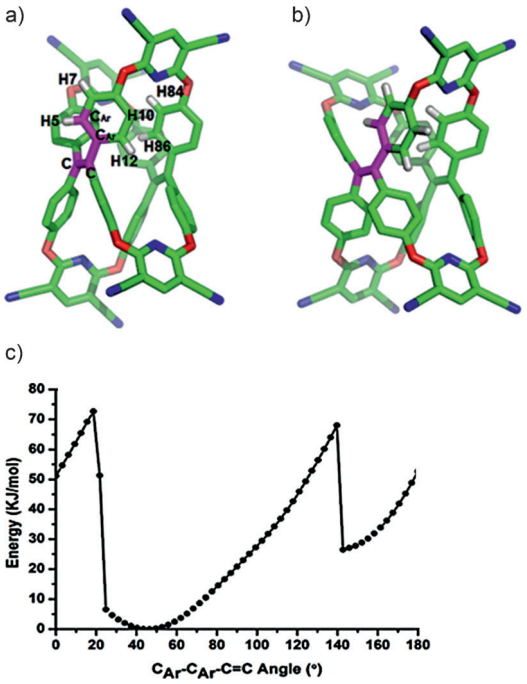

Figure 2. DFT-calculated structures of cage **1** with one phenyl ring fixed relative to other rings at 46.5° (a) and 18.6° (b). For clarity, some hydrogen atoms were omitted. Atom colors: N = blue; O = red; C = green. The purple-colored carbon atoms define the dihedral angles used to model the PESs. c) PES for the flipping of one phenyl ring in cage **1**.

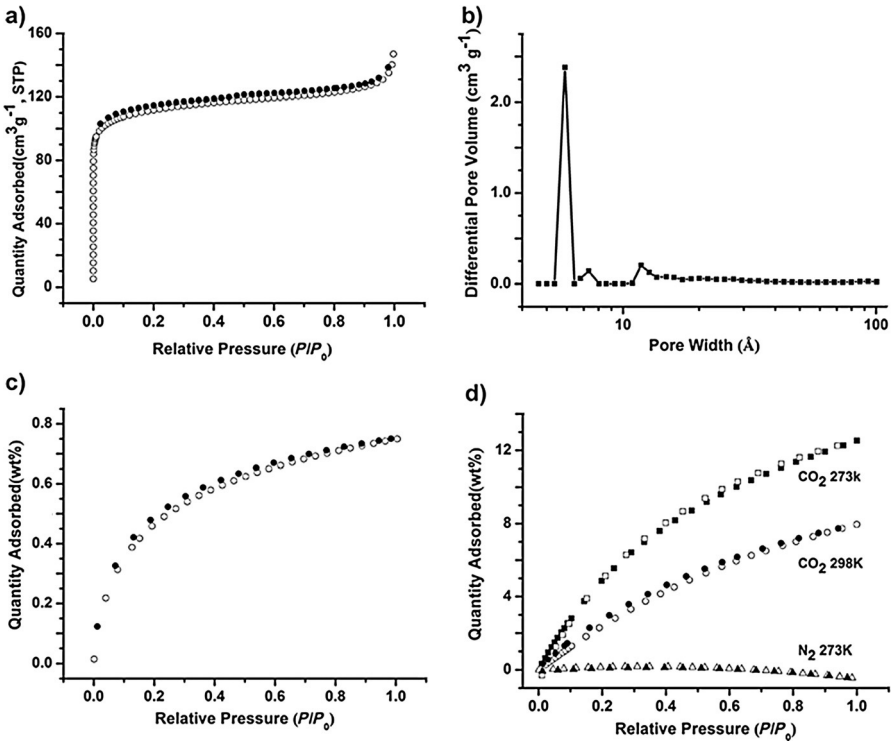

Figure 3. a) Nitrogen sorption isotherms of cage **1** at 77 K, b) pore size distributions calculated using the DFT method, c) H_2 sorption isotherms at 77 K, and d) CO_2 and N_2 sorption isotherms at 273 K and 298 K. In (a), (c), and (d), empty symbols denote gas adsorption and filled symbols denote desorption. STP = standard temperature and pressure.

nitrogen adsorption isotherms (Figure 3a) indicates that the structure has abundant micropores. The pore size distribution calculated by the DFT method (Figure 3b) also confirmed the presence of micropores with pore sizes of 5.8, 7.3, and 11.8 Å, which is in agreement with the crystallographic analysis (Figure 1). We compared the powder XRD patterns after the desolvation treatment with the calculated result (Figure S12) and deduced that cage **1** after desolvation is still in a microcrystalline state and has good thermal stability. Generally, ^{13}C cross-polarized magic angle spinning solid-state (CP-MAS) NMR spectroscopy can be utilized to probe molecular motion down to frequencies of circa 10^2 Hz.[39] The ^{13}C CP-MAS NMR spectra of cage **1** with and without solvent display signals with similar resolution and peak shape (Figure S13), which is consistent with slower rotation of the phenyl rings than what is detectable on the NMR timescale ($< 10^2$ Hz). This result is in agreement with the high energy barriers to rotation of the phenyl rings indicated by VT-NMR experiments and DFT calculations, and furthermore confirms that the empty crystals have permanent porosity.

Given the microporous structure and the polar functional groups of the pyridine rings and cyano groups, it was envisaged that cage **1** might also be suitable to adsorb H_2 and CO_2. As shown in Figure 3c, cage **1** can absorb 0.75 wt% of H_2 at 1.0 bar, which is similar to that found for TTEB at 10 bar.[5] The CO_2 sorption properties of cage **1** were measured at 273 K. As shown in Figure 3d, cage **1** can absorb 12.5 wt% (2.8 mmol g^{-1}) of CO_2 at 1.0 bar. With the moderate surface area, the good CO_2 uptake capacity of cage **1** is similar to the high CO_2 uptake reported by Schröder et al. for SOF-7 (12.54 wt%).[40] The uptake is also similar that reported by Cooper et al. for porous cages CC2 (3.0 mmol g^{-1}) and CC3 (2.5 mmol g^{-1}),[14] respectively, and is higher than the reported triptycene-based cages (11.0 wt% or 2.1 mmol g^{-1}) with high BET surface area of 1566 or 1700 $m^2 g^{-1}$, respectively.[15,18c] The excellent CO_2 adsorption ability of cage **1** may result from the perfect match of the microporous structure with the size of CO_2 and the electron-rich properties of nitrogen and oxygen atoms in the cage skeleton that facilitate local-dipole/quadrupole interactions with CO_2. The isosteric enthalpy (Q_{st}) of cage **1** toward CO_2 with a value of 24 kJ mol^{-1} was calculated from the adsorption isotherms at 273 K and 298 K using the Clausius–Clapeyron equation (Figure S14).[41] The selectivity of cage **1** toward CO_2 over N_2 was investigated by single-component gas sorption experiments at 273 K. A CO_2/N_2 selectivity of 80 was calculated from analysis of the initial slopes of the adsorption isotherms for cage **1** (Figure S15). The selectivity of cage **1** for CO_2/N_2 is much higher than most porous materials and comparable to some imine cages.[16,19]

In summary, we have designed and synthesized a quadrangular prismatic tricyclooxacalixarene cage **1** by a one-pot S_NAr condensation reaction. Cage **1** is a useful single-molecule platform to investigate the RIR mechanism of the AIE effect. For cage **1**, the TPE units were fixed by four pyridine rings in the tricyclooxacalixarene cage framework, which suppressed the motion or vibration of the phenyl rings with a high activation barrier for phenyl ring flipping. Therefore, the fluorescence of TPE was switched on in dilute solution. Moreover, cage **1** assembled into a grid-like porous structure in the solid state and exhibited an excellent adsorption capacity for CO_2 with high CO_2/N_2 selectivity. The ready accessibility of stable cage compounds might open new opportunities for the development of efficient cage-based porous materials in gas storage, catalysis, and chemosensors.

Keywords: aggregation-induced emission · cage compounds · calixarenes · gas storage · supramolecular chemistry

How to cite: *Angew. Chem. Int. Ed.* **2015**, *54*, 9244–9248
Angew. Chem. **2015**, *127*, 9376–9380

[1] a) A. P. Côté, A. I. Benin, N. W. Ockwig, M. O'Keeffe, A. J. Matzger, O. M. Yaghi, *Science* **2005**, *310*, 1166–1172; b) X. Feng, X. S. Ding, D. L. Jiang, *Chem. Soc. Rev.* **2012**, *41*, 6010–6022; c) S. Y. Ding, W. Wang, *Chem. Soc. Rev.* **2013**, *42*, 548–568.

[2] a) Y. H. Xu, S. B. Jin, H. Xu, A. Nagai, D. L. Jiang, *Chem. Soc. Rev.* **2013**, *42*, 8012–8031; b) S. Xu, Y. Luo, B. Tan, *Macromol. Rapid Commun.* **2013**, *34*, 471–484.

[3] a) B. Li, R. N. Gong, W. Wang, X. Huang, W. Zhang, H. M. Li, C. Hu, B. Tan, *Macromolecules* **2011**, *44*, 2410–2414; b) C. Zhang, Y. Liu, B. Li, B. Tan, C. F. Chen, H. B. Xu, X. L. Yang, *ACS Macro Lett.* **2012**, *1*, 190–193; c) Y. Luo, B. Li, W. Wang, K. Wu, B. Tan, *Adv. Mater.* **2012**, *24*, 5703–5707.

[4] a) P. Sozzani, A. Comotti, R. Simonutti, T. Meersmann, J. W. Logan, A. Pines, *Angew. Chem. Int. Ed.* **2000**, *39*, 2695–2698; *Angew. Chem.* **2000**, *112*, 2807–2810; b) P. Sozzani, S. Bracco, A. Comotti, L. Ferretti, R. Simonutti, *Angew. Chem. Int. Ed.* **2005**, *44*, 1816–1820; *Angew. Chem.* **2005**, *117*, 1850–1854.

[5] K. J. Msayib, D. Book, P. M. Budd, N. Chaukura, K. D. M. Harris, M. Helliwell, S. Tedds, A. Walton, J. E. Warren, M. Xu, N. B. McKeown, *Angew. Chem. Int. Ed.* **2009**, *48*, 3273–3277; *Angew. Chem.* **2009**, *121*, 3323–3327.

[6] Y. He, S. Xiang, B. Chen, *J. Am. Chem. Soc.* **2011**, *133*, 14570–14573.

[7] W. Yang, A. Greenaway, X. Lin, R. Matsuda, A. J. Blake, C. Wilson, W. Lewis, P. Hubberstey, S. Kitagawa, N. R. Champness, M. Schröder, *J. Am. Chem. Soc.* **2010**, *132*, 14457–14469.

[8] P. K. Thallapally, L. Dobrzańska, T. R. Gingrich, T. B. Wirsig, L. J. Barbour, J. L. Atwood, *Angew. Chem. Int. Ed.* **2006**, *45*, 6506–6509; *Angew. Chem.* **2006**, *118*, 6656–6659.

[9] H. Kim, Y. Kim, M. Yoon, S. Lim, S. Park, M. G. Seo, K. Kim, *J. Am. Chem. Soc.* **2010**, *132*, 12200–12202.

[10] a) A. Comotti, S. Bracco, P. Valsesia, M. Beretta, P. Sozzani, *Angew. Chem. Int. Ed.* **2010**, *49*, 1760–1764; *Angew. Chem.* **2010**, *122*, 1804–1808; b) S. Bracco, M. Beretta, A. Cattaneo, A. Comotti, A. Falqui, K. Zhao, C. Rogers, P. Sozzani, *Angew. Chem. Int. Ed.* **2015**, *54*, 4773–4777; *Angew. Chem.* **2015**, *127*, 4855–4859; c) A. Comotti, S. Bracco, A. Yamamoto, M. Beretta, T. Hirukawa, N. Tohnai, M. Miyata, P. Sozzani, *J. Am. Chem. Soc.* **2014**, *136*, 618–621.

[11] G. Zhang, M. Mastalerz, *Chem. Soc. Rev.* **2014**, *43*, 1934–1947.

[12] R. McCaffrey, H. Long, Y. Jin, A. Sanders, W. Park, W. Zhang, *J. Am. Chem. Soc.* **2014**, *136*, 1782–1785.

[13] Y. Jin, Q. Wang, P. Taynton, W. Zhang, *Acc. Chem. Res.* **2014**, *47*, 1575–1586.

[14] T. Tozawa, J. T. A. Jones, S. I. Swamy, S. Jiang, D. J. Adams, S. Shakespeare, R. Clowes, D. Bradshaw, T. S. Hasell, Y. Chong, C. Tang, S. Thompson, J. Parker, A. Trewin, J. Bacsa, A. M. Z. Slawin, A. Steiner, A. I. Cooper, *Nat. Mater.* **2009**, *8*, 973–978.

[15] M. Mastalerz, M. W. Schneider, I. M. Oppel, O. Presly, *Angew. Chem. Int. Ed.* **2011**, *50*, 1046–1051; *Angew. Chem.* **2011**, *123*, 1078–1083.

[16] Y. H. Jin, B. A. Voss, R. D. Noble, W. Zhang, *Angew. Chem. Int. Ed.* **2010**, *49*, 6348–6351; *Angew. Chem.* **2010**, *122*, 6492–6495.

[17] a) M. Liu, M. A. Little, K. E. Jelfs, J. T. A. Jones, M. Schmidtmann, S. Y. Chong, T. Hasell, A. I. Cooper, *J. Am. Chem. Soc.* **2014**, *136*, 7583 – 7586; b) T. Hasell, J. L. Culshaw, S. Y. Chong, M. Schmidtmann, M. A. Little, K. E. Jelfs, E. O. Pyzer-Knapp, H. Shepherd, D. J. Adams, G. M. Day, A. I. Cooper, *J. Am. Chem. Soc.* **2014**, *136*, 1438 – 1448.

[18] a) G. Zhang, O. Presly, F. White, I. M. Oppel, M. Mastalerz, *Angew. Chem. Int. Ed.* **2014**, *53*, 5126 – 5130; *Angew. Chem.* **2014**, *126*, 5226 – 5230; b) G. Zhang, O. Presly, F. White, I. M. Oppel, M. Mastalerz, *Angew. Chem. Int. Ed.* **2014**, *53*, 1516 – 1520; *Angew. Chem.* **2014**, *126*, 1542 – 1546; c) M. W. Schneider, I. M. Oppel, A. Griffin, M. Mastalerz, *Angew. Chem. Int. Ed.* **2013**, *52*, 3611 – 3615; *Angew. Chem.* **2013**, *125*, 3699 – 3703.

[19] Y. H. Jin, B. A. Voss, A. Jin, H. Long, R. D. Noble, W. Zhang, *J. Am. Chem. Soc.* **2011**, *133*, 6650 – 6658.

[20] J. S. Moore, *Acc. Chem. Res.* **1997**, *30*, 402 – 413.

[21] a) A. Avellaneda, P. Valente, A. Burgun, J. D. Evans, A. W. Markwell-Heys, D. Rankine, D. J. Nielsen, M. R. Hill, C. J. Sumby, C. J. Doonan, *Angew. Chem. Int. Ed.* **2013**, *52*, 3746 – 3749; *Angew. Chem.* **2013**, *125*, 3834 – 3837; b) C. Zhang, C. F. Chen, *J. Org. Chem.* **2007**, *72*, 9339 – 9341.

[22] Q. Wang, C. X. Zhang, B. C. Noll, H. Long, Y. H. Jin, W. Zhang, *Angew. Chem. Int. Ed.* **2014**, *53*, 10663 – 10667; *Angew. Chem.* **2014**, *126*, 10839 – 10843.

[23] M. X. Wang, H. B. Yang, *J. Am. Chem. Soc.* **2004**, *126*, 15412 – 15422.

[24] J. L. Katz, M. B. Feldman, R. R. Conry, *Org. Lett.* **2005**, *7*, 91 – 94.

[25] M. X. Wang, *Acc. Chem. Res.* **2012**, *45*, 182 – 195.

[26] H. Zhang, B. Yao, L. Zhao, D. X. Wang, B. Q. Xu, M. X. Wang, *J. Am. Chem. Soc.* **2014**, *136*, 6326 – 6332.

[27] J. L. Katz, K. J. Selby, R. R. Conry, *Org. Lett.* **2005**, *7*, 3505 – 3507.

[28] M. M. Naseer, D. X. Wang, L. Zhao, Z. T. Huang, M. X. Wang, *J. Org. Chem.* **2011**, *76*, 1804 – 1813.

[29] Y. N. Hong, J. W. Y. Lam, B. Z. Tang, *Chem. Soc. Rev.* **2011**, *40*, 5361 – 5388.

[30] a) C. W. T. Leung, Y. N. Hong, S. J. Chen, E. G. Zhao, J. W. Y. Lam, B. Z. Tang, *J. Am. Chem. Soc.* **2013**, *135*, 62 – 65; b) Z. K. Wang, S. J. Chen, J. W. Y. Lam, W. Qin, R. T. K. Kwok, N. Xie, Q. L. Hu, B. Z. Tang, *J. Am. Chem. Soc.* **2013**, *135*, 8238 – 8245; c) A. Bhunia, V. Vasylyeva, C. Janiak, *Chem. Commun.* **2013**, *49*, 3961 – 3963.

[31] a) H. T. Feng, Y. S. Zheng, *Chem. Eur. J.* **2014**, *20*, 195 – 201; b) M. Zhang, G. X. Feng, Z. G. Song, Y. P. Zhou, H. Y. Chao, D. Q. Yuan, T. T. Y. Tan, Z. G. Guo, Z. G. Hu, B. Z. Tang, B. Liu, D. Zhao, *J. Am. Chem. Soc.* **2014**, *136*, 7241 – 7244; c) Z. Wang, T. Y. Yong, J. S. Wan, Z. H. Li, H. Zhao, Y. B. Zhao, L. Gan, X. L. Yang, H. B. Xu, C. Zhang, *ACS Appl. Mater. Interfaces* **2015**, *7*, 3420 – 3425.

[32] G. Liang, J. W. Y. Lam, W. Qin, J. Li, N. Xie, B. Z. Tang, *Chem. Commun.* **2014**, *50*, 1725 – 1727.

[33] S. Song, H. F. Zheng, D. M. Li, J. H. Wang, H. T. Feng, Z. H. Zhu, Y. C. Chen, Y. S. Zheng, *Org. Lett.* **2014**, *16*, 2170 – 2173.

[34] a) Y. H. Xu, L. Chen, Z. Q. Guo, A. Nagai, D. L. Jiang, *J. Am. Chem. Soc.* **2011**, *133*, 17622 – 17625; b) Y. H. Xu, A. Nagai, D. L. Jiang, *Chem. Commun.* **2013**, *49*, 1591 – 1593.

[35] a) N. B. Shustova, B. D. McCarthy, M. Dincă, *J. Am. Chem. Soc.* **2011**, *133*, 20126 – 20129; b) N. B. Shustova, T. C. Ong, A. F. Cozzolino, V. K. Michaelis, R. G. Griffin, M. Dincă, *J. Am. Chem. Soc.* **2012**, *134*, 15061 – 15070.

[36] a) J. Q. Shi, N. Chang, C. H. Li, J. Mei, C. M. Deng, X. L. Luo, Z. P. Liu, Z. S. Bo, Y. Q. Dong, B. Z. Tang, *Chem. Commun.* **2012**, *48*, 10675 – 10677.

[37] C. Zhang, Z. Wang, S. Song, Y. S. Zheng, X. L. Yang, H. B. Xu, *J. Org. Chem.* **2014**, *79*, 2729 – 2732.

[38] M. Oki, *Applications of Dynamic NMR Spectroscopy to Organic Chemistry*, VCH, Weinheim, **1985**.

[39] W. Kolodziejski, J. Klinowski, *Chem. Rev.* **2002**, *102*, 613 – 628.

[40] J. Lü, C. Perez-Krap, M. Suyetin, N. H. Alsmail, N. H. Yan, S. Yang, W. Lewis, E. Bichoutskaia, C. C. Tang, A. J. C. R. Blake, M. Schröder, *J. Am. Chem. Soc.* **2014**, *136*, 12828 – 12831.

[41] V. Krungleviciute, L. Heroux, A. D. Migone, C. T. Kingston, B. Simard, *J. Phys. Chem. B* **2005**, *109*, 9317 – 9320.

[42] CCDC 1043021 (**1**) contains the supplementary crystallographic data for this paper. These data are provided free of charge by The Cambridge Crystallographic Data Centre.

Received: March 30, 2015
Revised: May 11, 2015
Published online: June 18, 2015

